Observation of Feshbach Resonances in an Ultracold Gas of ^{52}Cr

J. Werner, A. Griesmaier, S. Hensler, J. Stuhler, and T. Pfau*
5. Physikalisches Institut, Universität Stuttgart, 70550 Stuttgart, Germany

A. Simoni and E. Tiesinga
National Institute of Standards and Technology, Gaithersburg, Maryland 20899-8423, USA
(Received 2 December 2004; published 9 May 2005)

We have observed Feshbach resonances in collisions between ultracold ^{52}Cr atoms. This is the first observation of collisional Feshbach resonances in an atomic species with more than one valence electron. The zero nuclear spin of ^{52}Cr and thus the absence of a Fermi-contact interaction leads to regularly spaced resonance sequences. By comparing resonance positions with multichannel scattering calculations we determine the s-wave scattering length of the lowest $^{2S+1}\Sigma_g^+$ potentials to be 112(14) a_0, 58(6) a_0, and $-7(20)$ a_0 for $S = 6$, 4, and 2, respectively, where $a_0 = 0.0529$ nm.

DOI: 10.1103/PhysRevLett.94.183201 PACS numbers: 34.50.-s, 03.65.Nk, 31.10.+z

With the development of laser cooling and trapping techniques, atomic collisional properties in the ultracold regime have become directly accessible. Today, these properties play a crucial role in experiments with quantum degenerate bosonic and fermionic gases. In the ultracold regime, elastic collisions between most neutral atoms are dominated by isotropic interaction potentials, which only depend on the internuclear separation R and can be characterized by a single length, the s-wave scattering length a. This type of interaction is responsible for many of the fascinating phenomena observed in Bose-Einstein condensates (BEC's) (for a review see [1]) and two-species degenerate Fermi gases [2–5].

In alkali-metal gases, the effect of the isotropic potentials and, consequently, the value of the scattering length can be controlled by magnetically tunable Feshbach resonances [6]. Feshbach resonances appear when the energy of the incoming atoms equals the energy of a bound molecular level of a higher-lying molecular potential and can be used to change the sign and magnitude of a [7]. Recently, Feshbach resonances have been exploited to study the strong interaction regime in ultracold atomic gases or even to produce molecular Bose-Einstein condensates [7]. Feshbach resonances between different atomic species have also been theoretically predicted [8], and experimentally observed [9,10].

The spins of the six electrons in the $3d$ and $4s$ valence shells of the $^7S_3$ ground state of ^{52}Cr are aligned. This gives rise to a magnetic moment as large as $\mu = 6\mu_B$, where μ_B is the Bohr magneton. This large magnetic moment is responsible for a very strong anisotropic spin-spin dipole interaction between two $^7S_3$ ^{52}Cr atoms. In fact, when compared to alkali-metal atoms, which have a maximum magnetic moment of 1 μ_B, it is 36 times stronger.

For atomic ^{52}Cr the effects of the *anisotropic* and *long-range* spin-spin dipole interaction can add a new twist to the field of ultracold quantum gases. In particular, the expansion of a BEC of ^{52}Cr is expected to depend on the orientation of the magnetic dipoles [11]. The anisotropic interaction can be changed by time-varying magnetic fields [12], while the isotropic interaction can be tuned using a Feshbach resonance. This allows one to arbitrarily adjust the ratio of the isotropic and anisotropic interactions. One can thus create a so called dipolar quantum gas, in which the dipole-dipole interaction is dominant.

Isotropic interactions between two ground-state ^{52}Cr atoms can be described by Hund's case (a) $^{2S+1}\Sigma_{g/u}^+$ Born-Oppenheimer potentials. The large number of valence electrons leads to seven Born-Oppenheimer potentials instead of two for ground-state alkali-metal atoms. Conventional spectroscopic data only exists for the ground-state $^1\Sigma_g^+$ potential. Theoretical *ab initio* calculations [13,14] exist but are extremely challenging for ^{52}Cr.

Using a cross-dimensional relaxation technique, our group was able to determine the decatriplet $^{13}\Sigma_g^+$ s-wave scattering length of ^{52}Cr to be 170(39) a_0 and of ^{50}Cr to be 40(15) a_0 where $a_0 = 0.0529$ nm [15]. The uncertainty in parenthesis is a one standard deviation uncertainty combining statistical and systematic errors.

In this Letter, we report the observation of magnetic Feshbach resonances in a gas of ultracold ^{52}Cr atoms. We locate 14 resonances through inelastic loss measurements between magnetic-field values of 0 and 60 mT. The broadest observed feature has a $1/e$ width of 96 μT. By comparing the experimental data with theoretical multichannel calculations, we are able to identify the resonances and to determine the scattering lengths of the $^{13,9,5}\Sigma_g^+$ Born-Oppenheimer potentials, the van der Waals dispersion coefficient C_6, and C_8, which are the same for all seven Born-Oppenheimer potentials.

The details of our cooling scheme are presented in [16]. After Doppler cooling in a clover-leaf-type magnetic trap [16] and evaporative cooling, we load the atoms into a crossed optical dipole trap. The dipole trap is realized using an Yb-fiber laser with a wavelength of 1064 nm.

The two trapping beams have a waist of 30 and 50 μm and a power of 11 and 6 W, respectively. To suppress dipolar relaxation, we optically pump the atoms from the $m_s = +3$ Zeeman sublevel of the $^7S_3$ state to the energetically lowest $m_s = -3$ level [22]. The lifetime in the optical dipole trap increases from 7 s in the $m_s = +3$ state to 140 s in the $m_s = -3$ state and is limited by dipolar relaxation in the former and by the finite background gas pressure in the latter case. The optical pumping field of about 0.9 mT is left on, in order to prevent thermal reoccupation of higher m_s levels through dipolar collision processes. During the first 5 s after optical pumping, we see a fast initial decay in the atom number and a decrease in temperature, which we ascribe to plain initial evaporation in the optical dipole trap. To prepare a sample of up to 120 000 atoms at a temperature of 6 μK and a peak density of 5×10^{19} m^{-3} in a crossed optical dipole trap, we continue the evaporation by ramping down the intensity of the stronger of the two laser beams to 5 W.

We look for an increase of atom loss by three-body recombination to locate the Feshbach resonances [17]. This is done by first sweeping the magnetic-field strength in coarse steps on the order of 0.1–3 mT from 0 to 60 mT. Smaller sweep ranges are then used in regions where atom loss is observed. To find the precise location of the resonances a different method is used. The magnetic field is ramped up to a value close to the resonance in about 5 ms. We hold the magnetic field for 2 s to let the current settle and to give our magnetic coils time to thermalize. Then the magnetic field is quickly ramped to the desired value and held there for a variable amount of time. The holding time is chosen to clearly resolve the resonance and lies between 100 ms and 10 s. Finally, the magnetic field is switched off and an absorption image is taken.

The magnetic field is calibrated both slightly below and above each resonance using rf-spectroscopy. We are able to determine the value of the magnetic field with a one standard deviation uncertainty of 10 μT.

Figure 1 shows our data for two loss features near 29 mT. The position and widths of all the observed loss features are determined by a Gaussian fit, which we used for convenience. From the depth of these loss features, one can estimate an upper limit for the three-body loss coefficient L_3 [18]. The error bars in the figure are obtained from repeated measurements of atom loss and are mainly determined by number fluctuation. All resonance parameters are tabulated in Table I. In addition to atom loss, we also observe heating near most resonances, like in [18]. The resolution limit of our measurements is 14 μT at B = 60 mT.

Our experimental resonance positions can determine the scattering lengths of the Born-Oppenheimer potentials with high accuracy. The theoretical analysis uses the Hamiltonian of a pair of $^7S_3$ chromium atoms in an external magnetic field $\vec{B}$ and includes the seven isotropic Born-Oppenheimer potentials, the nuclear rotational energy $\hbar^2\vec{\ell}^2/(2\mu R^2)$ where $\vec{\ell}$ is the orbital angular momentum of the nuclei and μ the reduced mass of the diatom, the Zeeman interaction with the magnetic field, and the anisotropic spin-spin dipole interaction. For this Letter, we do not include second-order spin-orbit or spin-rotation interactions [19].

We construct $^{2S+1}\Sigma^+_{g/u}$ Born-Oppenheimer potentials V_S by smoothly joining a short-range $R \le R_x$ model potential with the well-known long-range dispersion potential $\sum_n -C_n/R^n$, in which we only retain the $n = 6$ and 8 terms. The connection point $R_x = 17.5\ a_0$ is chosen such that each V_S can be well represented by its long-range form beyond R_x and its value at R_x is much larger than the collision and bound-state energies of interest here. The inner wall and dissociation energy of the model potentials approximately agree with Ref. [14]. Details of the short-range potentials are unimportant at ultracold temperatures. We allow for variation of C_n and include short-range corrections near the minimum of each potential curve. This allows us to independently tune C_n and the s-wave scattering lengths a_S of V_S to fit the experimental data. The number of bound states of V_S is uncertain to ± 10 for the deeper potentials.

When the atoms are far apart, the eigenstates of the dimer are $|SM_S; \ell m_\ell\rangle$, in which M_S and m_ℓ are projections of $\vec{S}$ and $\vec{\ell}$ along $\vec{B}$. The total projection $M = m_\ell + M_S$ and parity $(-1)^\ell$ are conserved during the collision. As the nuclei of the atoms are identical, only states with $(-1)^{S+\ell} = 1$ exist. In absence of the spin-spin interaction, the Hamiltonian conserves $\vec{\ell}$ and $\vec{S}$ as well. The anisotropic spin-spin dipole interaction couples states with $\Delta S = 0, 2$ and $\Delta\ell = 0, 2$; with $\ell = 0 \rightarrow \ell' = 0$ transitions forbidden.

Our sample is spin polarized, so that the incoming state has quantum numbers $S = -M_S = 6$ by straightforward angular momentum addition. Moreover, the temperature of the sample, $T \approx 6\ \mu$K, is small compared to the $\ell \ge 2$

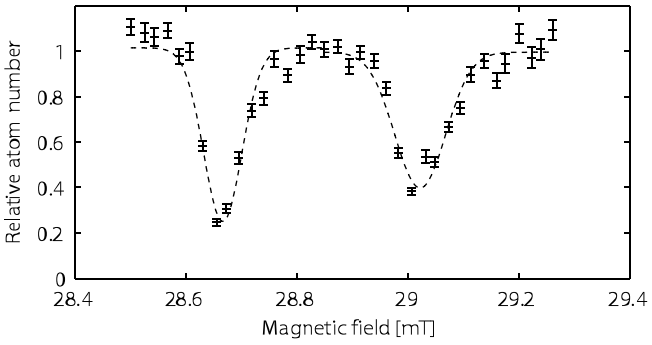

FIG. 1. Inelastic loss measurement of the Feshbach resonances at 28.66 and 29.03 mT. The dashed lines are Gaussian fits to the data and determine the position and width of the loss features. The experimental data points are averages over many experimental measurements. Each measurement was separately normalized to the offset of a Gaussian fit to the data.

TABLE I. Compendium of positions and strengths of the observed loss features L_3, the theoretical positions, widths Δ, initial partial wave ℓ_i, and assignment of the resonances. Theoretical calculations use a collision energy of $E = k_B T$ and parameters as in Fig. 2. The one standard deviation uncertainty of the experimental resonance position is below 14 μT (see text).

Exp. Pos. [mT]	Theo. Pos. [mT]	Theo. Δ [μT]	Upper limit for Exp. L_3 [m^6/s]	ℓ_i; SM_S; ℓm_ℓ
0.41	0.40	...	3×10^{-40}	2; 6, −4; 0, 0
0.61	...	...	8×10^{-41}	...
0.82	0.81	...	4×10^{-39}	2; 6, −5; 0, 0
5.01	5.01	$<1 \times 10^{-4}$	2×10^{-38}	0; 6, −2; 4, −4
6.51	6.49	6×10^{-4}	5×10^{-38}	0; 6, −3; 4, −3
9.89	9.85	0.030	1×10^{-36}	0; 6, −4; 4, −2
14.39	14.32	0.012	1×10^{-38}	0; 4, −2; 4, −4
18.83	18.79	0.022	4×10^{-38}	0; 4, −3; 4, −3
20.58	20.56	1.2	4×10^{-36}	0; 6, −5; 4, −1
28.66	28.80	1.2	6×10^{-37}	0; 4, −4; 4, −2
29.03	29.07	5.1	1×10^{-37}	0; 6, −4; 2, −2
37.92	37.92	0.042	1×10^{-37}	0; 2, −2; 4, −4
49.99	49.92	8.1	1×10^{-36}	0; 4, −4; 2, −2
58.91	58.92	170	3×10^{-36}	0; 6, −5; 2, −1

centrifugal barrier such that incoming $\ell_i = 0$ collisions dominate the scattering cross sections. We find that, in addition to the incoming state, states with $\ell = 2$ and 4 (d and g) partial waves and $S = 2, 4$, and 6 have to be coupled together in order to explain the 11 strongest observed features of Table I. Even though no term in the molecular Hamiltonian directly couples $\ell = 4$ states to the $\ell_i = 0$ state, second-order mixing in the spin-spin dipole interaction via $\ell = 2$ states is relevant in ^{52}Cr. All these states have a total projection $M = -6$. Two of the weakest $B <$ 1 mT resonances in Table I must be explained with incoming $\ell_i = 2$ d-wave collisions and $M \neq -6$.The resonance at 0.61 mT, the weakest observed resonance, could not be assigned.

The locations of the maxima in the experimental three-body loss rate are compared with locations of peaks in the elastic two-body cross section calculated by full quantum-scattering methods. We perform a global χ^2-minimization with parameters $a_{2,4,6}$, C_6, and C_8. Our best-fit parameters with one standard deviation are $a_2 = -7(20)\ a_0$, $a_4 = 58(6)\ a_0$, $a_6 = 112(14)\ a_0$, $C_6 = 733(70)$ a.u., and $C_8 = 75^{+90}_{-75} \times 10^3$ a.u. Here 1 a.u. is $E_h a_0^n$ for C_n and $E_h = 4.359\,744 \times 10^{-18}$ J is a Hartree. The minimization procedure provides only a weak upper bound on the C_8. The $^{13}\Sigma_g^+$ scattering length a_6 is in reasonable agreement with the C_6 coefficient is consistent with that of Ref. [14]. The average difference between theoretical and experimental resonance positions is only ≈ 0.06 mT.

Figure 2 shows the experimentally accessible s-wave scattering length a_{S,M_S} of two colliding $s = 3$, $m_s = -3$, ($S = -M_S = 6$) atoms as a function of magnetic field for our best-fit parameters. The theoretical resonance width Δ [6] is given in Table I. The experimental $1/e$ magnetic-field width of all observed features is on the order of 12–96 μT. Smaller experimental widths correspond to smaller theoretical widths, up to the point where we are limited by our experimental resolution of 14 μT. For resonances of a given S, increasing theoretical widths coincide with higher experimental L_3 values. The on-resonance loss rate we measure is comparable or smaller, respectively, than the ones observed in ^{23}Na [20] and ^{87}Rb [21]. This will allow for sufficient lifetimes for experiments in the vicinity of the resonance.

The nature of ^{52}Cr Feshbach resonances can be understood through approximate calculations of molecular bound states. We find that calculations of eigenstates of a reduced Hamiltonian limited to a single basis state $|SM_S; \ell m_\ell\rangle$ locates the resonances to within 0.25 mT from the scattering calculation. Our assignment S, M_S, ℓ, and m_ℓ from this approximate model is shown in Table I. An alternative assignment in which the quantum numbers of the nearly degenerate pair near 29.0 mT are interchanged is consistent with our best-fit parameters.

In the limit of vanishing spin-spin dipole interaction a simple resonance pattern is expected. Scattering is then independent of m_ℓ and the resonances occur at $B_{\rm res} = E_B/[g_s \mu_B (M_S + 6)]$, where E_B is one of the zero-field binding energies of the potential $V_S(R) + \hbar^2 \ell(\ell + 1)/(2\mu R^2)$. Inclusion of the spin-spin dipole interaction gives rise to observable deviations from this pattern, as large as ≈ 1 mT. Such shifts are an order of magnitude larger than the 0.06 mT discrepancies that remain after our least-squares fit. Moreover, the 0.06 mT agreement strongly suggests that the spin-spin dipole interaction is the dominant relativistic interaction in ultracold ^{52}Cr.

In conclusion, we have observed Feshbach resonances in an ultracold gas of ^{52}Cr atoms held in an optical dipole trap. Resonances were located by measuring the inelastic loss of ^{52}Cr in the energetically lowest Zeeman substate. Positions and widths extracted from quantum-scattering

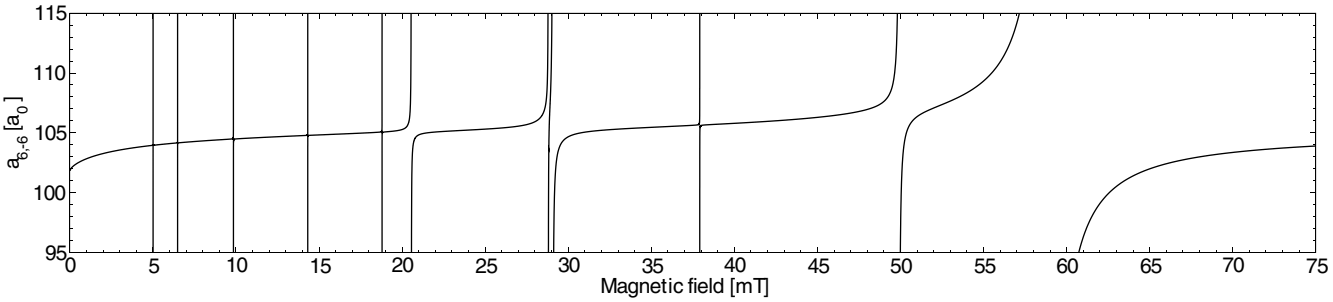

FIG. 2. Calculated scattering length of two $m_s = -3$ ^{52}Cr atoms versus magnetic field, for model parameters $a_6 = 111.56\ a_0$, $a_4 = 57.61\ a_0$, $a_2 = -7.26\ a_0$, $C_6 = 733$ a.u., and $C_8 = 75 \times 10^3$ a.u. The feature near 29 mT is a pair of nearly degenerate Feshbach resonances (see Fig. 1 for the corresponding experimental data).

calculations are in good agreement with the experimental data. The spin-spin dipole interaction is essential for a quantitative understanding of the experimental spectrum. We have improved the accuracy of the previous collisional measurements and provided a determination of the $^{9,5}\Sigma_g^+$ scattering lengths [15].

The resonances can be used to control the relative strength of isotropic and anisotropic interactions. Together with the BEC of ^{52}Cr we recently realized [22], this makes the spin-spin dipole interaction in degenerate quantum gases experimentally accessible. Moreover, the formation of Cr_2 molecules via Feshbach resonances is now envisaged.

This work is supported within the priority programme SPP 1116 of the DFG and the European RTN "Cold Quantum Gases" under Contract No. HPRN CT-2000-00125. We would like to thank A. Görlitz and S. Giovanazzi for many fruitful discussions.

*Electronic address: t.pfau@physik.uni-stuttgart.de

[1] K. Bongs and K. Sengstock, Rep. Prog. Phys. **67**, 907 (2004).
[2] C. Chin, M. Bartenstein, A. Altmeyer, S. Riedl, S. Jochim, J. H. Denschlag, and R. Grimm, Science **305**, 1128 (2004).
[3] T. Bourdel, L. Khaykovich, J. Cubizolles, J. Zhang, F. Chevy, M. Teichmann, L. Tarruell, S. J. J. M. F. Kokkelmans, and C. Salomon, Phys. Rev. Lett. **93**, 050401 (2004).
[4] M. Greiner, C. A. Regal, and D. Jin, Nature (London) **426**, 537 (2003).
[5] M. W. Zwierlein, C. A. Stan, C. H. Schunck, S. M. F. Raupach, A. J. Kerman, and W. Ketterle, Phys. Rev. Lett. **92**, 120403 (2004).
[6] E. Tiesinga, B. J. Verhaar, and H. T. C. Stoof, Phys. Rev. A **47**, 4114 (1993).
[7] R. A. Duine and H. T. C. Stoof, Phys. Rep. **396**, 115 (2004); and references therein.
[8] A. Simoni, F. Ferlaino, G. Roati, G. Modugno, and M. Inguscio, Phys. Rev. Lett. **90**, 163202 (2003).
[9] C. A. Stan, M. W. Zwierlein, C. H. Schunck, S. M. F. Raupach, and W. Ketterle, Phys. Rev. Lett. **93**, 143001 (2004).
[10] S. Inouye, J. Goldwin, M. L. Olsen, C. Ticknor, J. L. Bohn, and D. S. Jin, Phys. Rev. Lett. **93**, 183201 (2004).
[11] S. Giovanazzi, A. Görlitz, and T. Pfau, J. Opt. B **5**, S208 (2003).
[12] S. Giovanazzi, A. Görlitz, and T. Pfau, Phys. Rev. Lett. **89**, 130401 (2002).
[13] K. Andersson, Chem. Phys. Lett. **237**, 212 (1995).
[14] Z. Pavloviç, B. O. Roos, R. Côté, and H. R. Sadeghpour, Phys. Rev. A **69**, 030701 (2004).
[15] P. O. Schmidt, S. Hensler, J. Werner, A. Griesmaier, A. Görlitz, and T. Pfau, Phys. Rev. Lett. **91**, 193201 (2003).
[16] P. O. Schmidt, S. Hensler, J. Werner, T. Binhammer, A. Görlitz, and T. Pfau, J. Opt. Soc. Am. B **20**, 960 (2003).
[17] J. Stenger, S. Inouye, M. R. Andrews, H.-J. Miesner, D. M. Stamper-Kurn, and W. Ketterle, Phys. Rev. Lett. **82**, 2422 (1999).
[18] T. Weber, J. Herbig, M. Mark, H.-C. Nagerl, and R. Grimm, Phys. Rev. Lett. **91**, 123201 (2003).
[19] H. Lefebvre-Brion and R. W. Field, *Perturbations in the Spectra of Diatomic Molecules* (Academic, London, 1986).
[20] J. Stenger, S. Inouye, M. R. Andrews, H.-J. Miesner, D. M. Stamper-Kurn, and W. Ketterle, Phys. Rev. Lett. **82**, 2422 (1999).
[21] J. L. Roberts, N. R. Claussen, S. L. Cornish, and C. E. Wieman, Phys. Rev. Lett. **85**, 728 (2000).
[22] A. Griesmaier, J. Werner, S. Hensler, J. Stuhler, and T. Pfau, Phys. Rev. Lett. **94**, 160401 (2005).